Low-Order Output Feedback Compensator for Tracking Systems

C. B. Asthana,* M. Seetharama Bhat,† and K. N. Swamy‡
Indian Institute of Science, Bangalore 560012, India

Introduction

THE synthesis of a compensator using the output feedback is a problem of great practical importance and has received wide attention in the past two decades.[1] The quadratic optimal fixed-order output feedback dynamic compensator is designed by iteratively solving the necessary conditions for optimality.[2] The same formulation is used for designing static gain or dynamic compensator. It has been shown[3] that, if we start with a stabilizing initial compensator, the iteration converges to a local minimum and that the local minimum depends on the starting value.[4] Several methods that offer the initial stabilizing gains are quoted in Ref. 5. In Ref. 6, a linear quadratic Gaussian (LQG) solution for the reduced-order plant is taken as the initial value. Here, too, we find the LQG solution for the initial compensator. But our method differs from all of the previous methods in many ways. First, we use a general structure of the compensator in which all of the elements are adjustable through optimization. Second, we take a tracking system described by physical variables and choose the feedback loop for the LQG design such that it is equivalent to the dynamic compensator in the feedforward loop. Third, we reduce the order of the compensator to an acceptable low order. Starting with this, we find the optimal compensator using the approximate loop transfer recovery (LTR) technique.[4] This Note is concerned with finding the initial values for the compensator parameters, reducing its order, and then obtaining the low-order optimal dynamic compensator by applying LTR technique for approximately recovering the full-state loop matrix at the plant input. The method is applied to the design of autopilot for a surface-to-air missile.

Autopilot Configuration

The linear time invariant description of the pitch plane dynamics of a missile is given by

$$\dot{\boldsymbol{x}} = A\boldsymbol{x} + Bu, \qquad u \in R^m \tag{1}$$

$$y = C\boldsymbol{x} + Du, \qquad y \in R^p \tag{2}$$

$$y_t = C_t\boldsymbol{x} + D_t u, \qquad y_t \in R^p \tag{3}$$

$$y_f = C_f\boldsymbol{x}, \qquad y_f \in R^r \tag{4}$$

The variable y is the controlled output, and y_t and y_f are the outputs used for command tracking and feedback stabilization, respectively. It is assumed that the pair (C_f, A) is observable. Therefore, y_f is used as an input to dynamic compensator with the Kalman filter as an initial configuration. Let the dynamic compensator $[G_c(s)]$, shown in Fig. 1, be described as $\dot{\boldsymbol{x}}_c = A_c\boldsymbol{x}_c + B_c u_c$ and $u = C_c\boldsymbol{x}_c + D_c u_c$, where $u_c = [y_f \;\; e]'$. Corresponding to the inputs, the matrices B_c and D_c are partitioned as $[B_c^f \;\; B_c^t]$ and $[D_c^f \;\; D_c^t]$, respectively. The tracking error dynamics can be written as $\dot{e} = \bar{R} - y_t$. The augmented plant dynamics can be described as

$$\begin{bmatrix} \dot{\boldsymbol{x}} \\ \dot{e} \\ \dot{\boldsymbol{x}}_c \end{bmatrix} = \begin{bmatrix} A + BD_c^f C_f & BD_c^t & BC_c \\ -C_t - D_t D_c^f C_f & -D_t D_c^t & -D_t C_c \\ B_c^f C_f & B_c^t & A_c \end{bmatrix} \begin{bmatrix} \boldsymbol{x} \\ e \\ \boldsymbol{x}_c \end{bmatrix} + \begin{bmatrix} 0 \\ I \\ 0 \end{bmatrix} \bar{R} \tag{5}$$

which can be written in the standard output feedback form as

$$\dot{\bar{\boldsymbol{x}}} = (\bar{A} + \bar{B}\bar{G}\bar{C})\bar{\boldsymbol{x}} + \bar{B}_r\bar{R} \tag{6}$$

where

$$\bar{A} = \begin{bmatrix} A & 0 & 0 \\ -C_t & 0 & 0 \\ 0 & 0 & 0 \end{bmatrix}, \qquad \bar{B} = \begin{bmatrix} B & 0 \\ -D_t & 0 \\ 0 & I \end{bmatrix}$$

$$\bar{C} = \begin{bmatrix} C_f & 0 & 0 \\ 0 & I & 0 \\ 0 & 0 & I \end{bmatrix}, \qquad \bar{G} = \begin{bmatrix} D_c^f & D_c^t & C_c \\ B_c^f & B_c^t & A_c \end{bmatrix}$$

$$\bar{\boldsymbol{x}} = [\boldsymbol{x} \quad e \quad \boldsymbol{x}_c]'$$

Here all of the known quantities are combined in $\bar{A}$, $\bar{B}$, and $\bar{C}$, and all of the unknown parameters are in $\bar{G}$.

Equivalent LQG Solution for Initial Gains

The initial stabilizing compensator is found by the LQG solution of an equivalent configuration (Fig. 1), which can be represented as

$$\begin{bmatrix} \dot{\boldsymbol{x}} \\ \dot{e} \\ \dot{\hat{\boldsymbol{x}}} \end{bmatrix} = \begin{bmatrix} A & BK_2 & BK_1 \\ -C_t & -D_t K_2 & -D_t K_1 \\ K_f C_f & BK_2 & A - K_f C_f + BK_1 \end{bmatrix} \begin{bmatrix} \boldsymbol{x} \\ e \\ \hat{\boldsymbol{x}} \end{bmatrix} + \begin{bmatrix} 0 \\ I \\ 0 \end{bmatrix} \bar{R} \tag{7}$$

In Eq. (7), $\hat{\boldsymbol{x}}$ is the estimated state vector and $\dot{\hat{\boldsymbol{x}}}$ is its time derivative. K_1 and K_2 are the full state feedback corresponding to the plant state $\boldsymbol{x}$ and the integrator state e, respectively. K_f is the Kalman filter gain. Now comparing Eqs. (5) and (7), we get

$$\begin{bmatrix} D_c^f & D_c^t & C_c \\ B_c^f & B_c^t & A_c \end{bmatrix} = \begin{bmatrix} 0 & K_2 & K_1 \\ K_f & BK_2 & A - K_f C_f + BK_1 \end{bmatrix} = \bar{G} \tag{8}$$

Optimal Solution for Approximate Loop Recovery

The necessary condition for minimization[2] of the performance index

$$J(A_c, B_c, C_c, D_c) = E_{x_0}\left[\int_0^\infty [\boldsymbol{x}'Q\boldsymbol{x} + u_c'Ru_c]\,\mathrm{d}t\right] \tag{9}$$

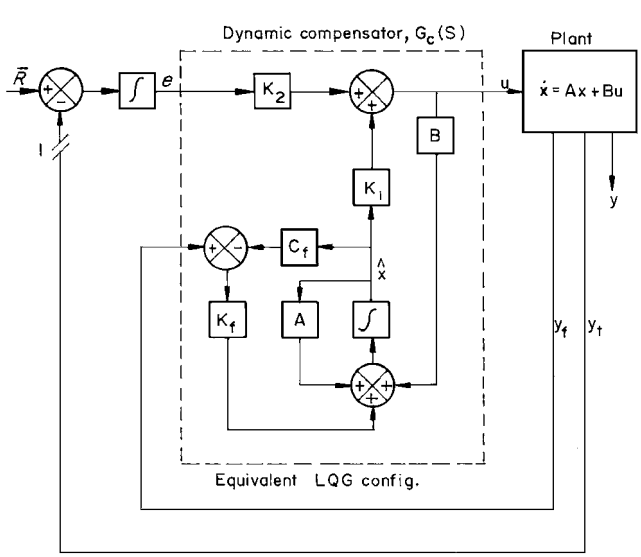

Fig. 1 Autopilot configuration.

Received Nov. 15, 1996; revision received May 20, 1997; accepted for publication June 1, 1997.

*Research Student, Department of Aerospace Engineering. Member AIAA.
†Associate Professor, Department of Aerospace Engineering. E-mail: msbdcl@aero.iisc.ernet.in.
‡Scientist, Advanced Technology Programme.

requires the solution of the triple G, K, L satisfying

$$KM + M'K + Q + \bar{C}'\bar{G}'R\bar{G}\bar{C} = 0 \tag{10}$$

$$LM' + ML + X_0 = 0 \tag{11}$$

$$\bar{G}\bar{C}L\bar{C}' + R^{-1}\bar{B}'KL\bar{C}' = 0 \tag{12}$$

for a stable closed-system matrix $M = \bar{A} + \bar{B}\bar{G}\bar{C}$. In Eq. (11), X_0 is the variance matrix assumed for the initial state x_0, which can be taken as diag($[BB'; x^0]$), where x^0 is small positive value corresponding to the compensator states. At the plant input, the return signal from the full-state feedback is $u^* = K_1^* x + K_2^* e$ and that from the reduced-order compensator is $u_r = C_{cr}\boldsymbol{x}_{cr} + D_{cr}^f C_f \boldsymbol{x} + D_{cr}^t e$. (The subscript r stands for reduced order.) For LTR, the objective is to minimize error $y_1 = u^* - u_r$, which leads to the following index of performance[4]:

$$J = E_{x_0}\left[\int_0^\infty [y_1' y_1 + \rho u_c' u_c]\,\mathrm{d}t\right] \tag{13}$$

By defining Q_1 as $[(K_1^* - D_{cr}^f C_f), (K_2^* - D_{cr}^t), -C_{cr}]$, we get $Q = Q_1' Q_1$ and $R = \rho I_m$ for Eq. (9). Here the plant states are $[\boldsymbol{x}, e, \boldsymbol{x}_{cr}]'$. Taking the preceding as the initial value, the optimal compensator is computed.

Autopilot Design Example

The missile has wing (δ_w) and tail (δ_t) as two independent inputs. Here y_t is sensed pitch (lateral) acceleration, i.e., latax, y_f is sensed pitch rate q, and y is the latax at the center of gravity. The autopilot is required to track only the latax with the rise time of about 0.2 s and the overshoot and tracking accuracy of less than 10 and 5%, respectively. The outer tracking loop is single input/single output (SISO). The robustness requirement for the SISO loop broken at point 1 in Fig. 1 is better than 6 dB and 30 deg for gain and phase margins, respectively, with greater than 40-dB/decade rolloff. The data are based on Ref. 7. The pitch dynamics without actuators is described as

$$A = \begin{bmatrix} 0 & 1 & 0 \\ 0 & -0.39 & -576.367 \\ 0.0056 & 0.999 & -1.2902 \end{bmatrix}$$

$$B = \begin{bmatrix} 0 & 0 \\ -285.2 & 115.0 \\ 0.2239 & 0.0995 \end{bmatrix}, \qquad C_t = [0 \quad -0.084 \quad -858.213]$$

$$D_t = [303.08 \quad 38.0], \qquad C = [0 \quad -0.24 \quad -1088.8]$$

$$D = [189.0 \quad 84], \qquad C_f = [0 \quad 1 \quad 0]$$

The plant state vector $\boldsymbol{x} = [\theta$ (attitude), q (pitch rate), α (angle of attack)$]'$. The wing and the tail have second-order actuators ($\omega_n = 90$ rad/s, $\zeta = 0.7$ and $\omega_n = 150$ rad/s, $\zeta = 0.7$, respectively). The transmission zeros for the two-input/two-output plant are at -6.78×10^{-21} and -1.77×10^{-4}. The open-loop eigenvalues are $(-0.00556, -0.84 \pm 23.99j)$. To find a low-order initial compensator, the plant without actuators is considered. After augmenting the plant with the integrator (Fig. 1), linear quadratic regulator (LQR) design is carried out with the weighting matrices as $Q = \mathrm{diag}([0.001; 0.01; 0.01; 0.0005])$ and $R = I_2$. The weights corresponding to q and α are selected higher so that the speed of response and damping are satisfactory. The speed of step response and steady-state accuracy are improved by selecting nonzero weight on e. The weight on θ is kept an order lower than that on q. For the Kalman filter design, the process noise covariance matrix is chosen as diag($[0.05; 0.05; 0.0025]$), which is higher than Q selected for LQR, to get faster filter dynamics. Based on the noise characteristics of the rate gyro, the measurement noise covariance is chosen as 10^{-2}. Here the aim is to get only an initial stabilizing compensator. The corresponding gain matrices are

$$K_1 = \begin{bmatrix} 0.0006 & 0.1080 & 1.1761 \\ -0.0003 & -0.0398 & -0.1395 \end{bmatrix}, \qquad K_2 = \begin{bmatrix} 0.0223 \\ -0.0012 \end{bmatrix}$$

The Kalman filter gain matrix $K_f = [-1.4495, 10.3241, -0.0951]'$. A third-order (same as that of the plant) compensator is obtained from Eq. (8), which is then reduced, using Hankel norm minimization,[8] to a first order (G_c) given as

$$A_{cr} = [-95.0403], \qquad B_{cr} = [10.4414, -5.1727]$$

$$C_{cr} = \begin{bmatrix} 0.2545 \\ -0.0595 \end{bmatrix}, \qquad D_{cr} = \begin{bmatrix} 0 & 0.0223 \\ 0 & -0.0012 \end{bmatrix}$$

We now apply approximate LTR technique to get the optimal compensator. For this, full-state feedback gains K_1^* and K_2^* (Fig. 1) are worked out for the full-order plant with states as $\boldsymbol{x} = [\theta, q, \alpha, \delta_w, \dot{\delta}_w, \delta_t, \dot{\delta}_t, e]'$. In this case, $Q = \mathrm{diag}([0.001; 0.01; 0.01; 10^{-5}; 10^{-5}; 10^{-5}; 10^{-5}; 0.0005])$ and $R = I_2$ are chosen. Note that very low (10^{-5}) weights corresponding to the actuator states are added (because there is no need to move them) and the rest of the weights are the same as before. The feedback gain matrices obtained are

$$K_1^* = \begin{bmatrix} 0.0007 & 0.1168 & 0.4301 & -0.5994 & -0.0044 & 0.1213 & 0.0005 \\ -0.0003 & -0.0482 & 0.0375 & 0.2172 & 0.0014 & -0.0529 & -0.0007 \end{bmatrix}, \qquad K_2^* = \begin{bmatrix} 0.0222 \\ -0.0027 \end{bmatrix}$$

The optimal compensator found as

$$A_c = [-74.3922], \qquad B_c = [8.1257, -3.9665]$$

$$C_c = \begin{bmatrix} 2.4211 \\ 6.7860 \end{bmatrix}, \qquad D_c = \begin{bmatrix} -0.2177 & 0.1583 \\ -0.8894 & 0.4098 \end{bmatrix}$$

gives the closed-loop eigenvalues as $[-0.01, -65.02, -188.92, -42.01 \pm 137.78j, -23.1 \pm 42.19j, -14.12 \pm 9.48j]$. Note that, with the reduced-order compensator, full recovery is not possible.[4] In this example, ρ could not be reduced below 0.3 without increasing overshoots in the step response. However, the compensator thus obtained offers a practically acceptable design, as shown by the step response in Fig. 2. The control deflections are 0.1 and 0.25 deg for δ_w and δ_t, respectively. The gain and phase margins obtained are 17 dB and 90 deg, respectively, with about 40-dB/decade rolloff. The robustness check with 30% variation in moment and force coefficients give 2% overshoot in the step response and a 1-dB decrease in the gain margin along with a 2-deg decrease in the phase margin.

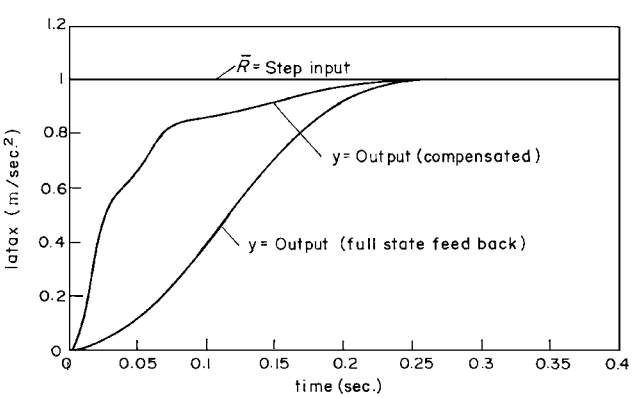

Fig. 2 Time history for a step latax command input.

Conclusion

A method is developed to find the initial stabilizing low-order output feedback dynamic compensator by using the LQG solution for an equivalent configuration and reducing the order. The compensator found by employing an approximate LTR technique offers a design with good performance.

References

[1]Syrmos, V. L., Abdallah, C., Dorato, P., and Grigoriadis, K., "Static Output Feedback—A Survey," *Automatica*, Vol. 33, No. 2, 1997, pp. 125–137.

[2]Levine, W. S., and Athans, M., "On the Determination of the Optimal Constant Output Feedback Gains for Linear Multivariable Systems," *IEEE Transactions on Automatic Control*, Vol. 15, No. 1, 1970, pp. 44–48.

[3]Moerder, D. D., and Calise, A. J., "Convergence of Numerical Algorithm for Calculating Optimal Output Feedback Gains," *IEEE Transactions on Automatic Control*, Vol. 30, No. 1, 1985, pp. 900–903.

[4]Calise, A. J., and Prasad, J. V. R., "Approximate Loop Transfer Recovery Method for Designing Fixed-Order Compensators," *Journal of Guidance, Control, and Dynamics*, Vol. 13, No. 2, 1990, pp. 297–302.

[5]Kucera, V., and DeSouza, C. E., "A Necessary and Sufficient Condition for Output Feedback Stabilizability," *Automatica*, Vol. 31, No. 9, 1995, pp. 1357–1359.

[6]Mukhopadhyay, V., Newsom, J. R., and Abel, I., "Reduced-Order Optimal Feedback Control Law Synthesis for Flutter Suppression," *Journal of Guidance, Control, and Dynamics*," Vol. 5, No. 4, 1982, pp. 50–54.

[7]Nichols, J. O., "Analysis and Compilation of Missile Aerodynamic Data, Volume 1, Data Presentation and Analysis," NASA CR-2835, May 1977.

[8]Sofonov, M. G., and Chiang, R. Y., "Robust Control Tool Box for Use with MATLAB," *User's Guide*, MathWorks, Natick, MA, 1986.

Dynamics of a Dual-Probe Tethered System

Joshua Ashenberg* and Enrico C. Lorenzini†
Harvard–Smithsonian Center for Astrophysics, Cambridge, Massachusetts 02138

I. Introduction

THE concept of a multiprobe tether has been recently proposed as a feasible configuration for a mission to collect data in the lower thermosphere.[1] Such a mission would be extremely valuable to atmospheric scientists who need to understand the cooling processes of the lower thermosphere, which are linked to global warming of the troposphere and ozone depletion in the stratosphere. The altitude of interest, 120–150 km, is not accessible to balloons or satellites. The atmosphere in this region is too rarefied for balloons and too dense for satellites. A long tether would allow probes to be lowered deep into the atmosphere from an orbiter positioned above. The multiprobe configuration offers the opportunity to measure the vertical gradient of the atmospheric properties under investigation. There are also other interesting applications for long tethers, such as wind-tunnel experiments under actual conditions and stereoscopic remote sensing of the Earth's surface.[2]

This Note treats the dynamics of a dual probe, where two probes, close to each other, are located at the far end of the tether. The system is designed to operate at the desired low altitudes and keep the tether oscillations bounded and small. The purpose of this research is to gain a preliminary understanding of the system dynamics suitable for a feasibility study and to select preliminary values of parameters for further investigation. The guideline of the research is to examine the influence of the various parameters on the system stability, assuming that the system starts from stable conditions (particularly, zero amplitude and zero rate). Small perturbations and modal analysis techniques are applied for analyzing the linear, i.e., small amplitude, motion. The nonlinear motion is analyzed by means of a systematic parametric study that uses numerical simulations and stroboscopic mapping techniques.

Received May 2, 1996; revision received April 18, 1997; accepted for publication June 20, 1997.

*Consultant, Radio and Geoastronomy Division, Mail Stop 80. Member AIAA.

†Staff Scientist, Radio and Geoastronomy Division, Mail Stop 80. Senior Member AIAA.

II. Model

The system under investigation consists of two small probes, m_1 and m_2, attached to a tether connected to a massive orbiter with mass M and orbital radius r. The tether length between the orbiter and the first probe is L_1, and the length between the probes is L_2. Typically $m_1 = 200\,\text{kg}, m_2 = 40\text{–}200\,\text{kg}$, and $M = 90{,}000\,\text{kg}$. Thus, the typical value of the probe mass ratio is $0.2 \le \epsilon_m \le 1$, where $\epsilon_m = m_2/m_1$. The second dimensionless parameter is the length ratio, defined as $\epsilon_L = L_2/L_1$. The length of the dual tether is about 100 km $(L_1 + L_2)$. Because L_2 typically is shorter than the local atmospheric scale height, i.e., 5 km, ϵ_L is a small parameter, i.e., $\epsilon_L \ll 1$. The orbiter moves in a small eccentricity orbit $(e < 0.01)$ around the Earth at an altitude of 220–250 km. Therefore, although the orbiter may be considered as drag-free for the duration of the mission, the atmospheric perturbations are significant when dealing with the dynamics of the probes. Generally speaking, the system dynamics is extremely complicated and requires tedious modeling and simulations. Because this research is primarily a parametric investigation, a reasonable model reduction must be applied to identify the characteristic dynamic behavior of the system. The main assumptions are that all satellites are in a single orbital plane, the satellites are point masses, and the tether is inelastic and massless. These are classic assumptions adopted by many authors working on tethered systems.[3]

The desired equations for the pitch tether angles α_1 and α_2 in terms of the true anomaly θ as the independent variable are derived from the Lagrangian function $L = K - V$. The kinetic energy K and the potential energy V are as follows:

$$\begin{aligned} K &= \tfrac{1}{2}MV_M^2 + \tfrac{1}{2}m_1\left(V_1^2 + \epsilon_m V_2^2\right) \\ &= \tfrac{1}{2}[M + (1+\epsilon_m)m_1](\dot r^2 + r^2\dot\theta^2) + \tfrac{1}{2}m_1\Big[L_1^2(1+\epsilon_m) \\ &\quad \times (\dot\alpha_1 + \dot\theta)^2 + 2L_1(1+\epsilon_m)(\dot\alpha_1 + \dot\theta)(\dot r\sin\alpha_1 - r\dot\theta\cos\alpha_1) \\ &\quad + \epsilon_m L_2^2(\dot\alpha_2 + \dot\theta)^2 + 2\epsilon_m L_2(\dot\alpha_2 + \dot\theta)(\dot r\sin\alpha_2 - r\dot\theta\cos\alpha_2) \\ &\quad + 2\epsilon_m L_1 L_2(\dot\alpha_1 + \dot\theta)(\dot\alpha_2 + \dot\theta)\cos(\alpha_1 + \alpha_2)\Big] \end{aligned} \tag{1}$$

and

$$\begin{aligned} V &= -\mu_\oplus\left[\frac{M}{r} + m_1\left(\frac{1}{r_1} + \frac{\epsilon_m}{r_2}\right)\right] \\ &= -\frac{\mu_\oplus M}{r} - \frac{\mu_\oplus(1+\epsilon_m)m_1}{r}\left[1 + \frac{L_1}{r}\cos\alpha_1\right. \\ &\quad \left. - \frac{1}{2}\frac{L_1^2}{r}\left(1 - 3\cos^2\alpha_1\right) + \frac{\epsilon_m}{1+\epsilon_m}\frac{L_2}{r}\cos\alpha_2 + O\left(\frac{L_1L_2}{r^2}\right)\right] \end{aligned} \tag{2}$$

where V_j represents the velocity of the j mass and $(\dot{})$ are time derivatives. Equation (2) is a result of a small-length ratio expansion, where terms of orders of magnitude $\{(L_1/r)^3 < L_1L_2/r^2\} \ll (L_1/r)^2$ are neglected. The equations of motion derived from the Lagrangian function are then expressed in terms of the true anomaly as follows:

$$\begin{aligned} &\left(1 + \epsilon_m\sin^2\Delta\alpha\right)(1 + e\cos\theta)\alpha_1'' - 2\left(1 + \epsilon_m\sin^2\Delta\alpha\right)e\sin\theta\alpha_1' \\ &\quad + \frac{1}{2}\epsilon_m(1 + e\cos\theta)(\alpha_1' + 1)^2\sin 2\Delta\alpha \\ &\quad + \epsilon_m\epsilon_L(1 + e\cos\theta)(\alpha_2' + 1)^2\sin\Delta\alpha \\ &\quad - 2\epsilon_m e\sin\theta\sin^2\Delta\alpha + \frac{3}{2}(1+\epsilon_m)\sin 2\alpha_1 \\ &\quad = 2e\sin\theta + \frac{r^3}{\mu_\oplus}\frac{1}{m_1L_1^2}\left(Q_{\alpha_1} - \frac{\cos\Delta\alpha}{\epsilon_L}Q_{\alpha_2}\right) \end{aligned} \tag{3}$$